The Effects of Intermittent Aeration on the Characteristics of Bio-Cake Layers in a Membrane Bioreactor

ARTICLE *in* ENVIRONMENTAL SCIENCE AND TECHNOLOGY · OCTOBER 2007

Impact Factor: 5.33 · DOI: 10.1021/es070467a · Source: PubMed

Environ. Sci. Technol. **2007**, *41,* 6270−6276

The Effects of Intermittent Aeration on the Characteristics of Bio-Cake Layers in a Membrane Bioreactor

SEOK-HWAN HONG,[†] WOO-NYOUNG LEE,[†] HYUN-SUK OH,[†] KYUNG-MIN YEON,[†] BYUNG-KOOK HWANG,[†] CHUNG-HAK LEE,*[,†] IN-SOUNG CHANG,[‡] AND SANGHO LEE[§]

School of Chemical and Biological Engineering, Seoul National University, Seoul 151-744, Korea, Department of Environmental Engineering, Hoseo University, Asan, Chung-Nam, 336-795, Korea, and Construction Environment Research Department, Korea Institute of Construction Technology, Ilsan, Kyunggi-do 411-712, Korea

The effects of a sequencing variation for dissolved oxygen (DO) concentrations on the membrane permeability in a submerged membrane bioreactor (MBR) were studied. An MBR was continuously operated under alternating DO conditions, e.g., 36 h of an aerobic phase, followed by 36 h of an anoxic phase. The rate of increase in transmembrane pressure (TMP) in the anoxic phase was always steeper than that in the aerobic phase, indicating that the fouling rate was higher in the anoxic than in the aerobic condition. Regardless of the phases, the rate of TMP increase became steeper as the cycles were repeated. However, this trend became less important as the cycle numbers increased. Even in identical microbial communities, the number of colloidal particles and soluble extracellular polymeric substances (EPS) in the bulk solution were increased during the anoxic condition, which caused a reduction in the porosity of the bio-cake. During analysis of the bio-cake profile along the cake depth, the temporal variation of the bio-cake structure was attributed to the temporal change in the number of colloidal particles as well as the change in compression forces acting on the bio-cake. The influence of the latter was found to be more important than that of the former, which was verified by comparing the various structures of bio-cake formed in differing DO environments.

Introduction

Recently, a combination of membrane technologies with biological nutrient removal (BNR) processes has been widely practiced because membrane-coupled BNR (m-BNR) processes have many advantages over conventional BNR processes, such as a high rate of organic removal, particle-free effluent, and a small footprint (*1*).

The m-BNR processes employ anoxic and/or anaerobic tanks as well as aeration basins for successful denitrification and phosphorus uptake (*2*). Thus, microorganisms in m-BNR processes repeatedly encounter aerobic and anoxic conditions along the internal recycle line. Microorganisms in a membrane-coupled sequencing batch reactor (m-SBR) are also exposed to different dissolved oxygen (DO) concentrations (*3*).

In m-BNR and m-SBR, as microorganisms are repeatedly exposed to conditions that alternate between aerobic and anoxic or anaerobic, they are likely to be stressed due to the change in DO levels, which might affect membrane filterability. Some studies have been carried out on the effect of oxygen level on membrane permeability (*4*−*6*). These studies compared the membrane filterability of two separate reactors operating under different oxygen conditions. They reported that the membrane fouling was greater in the anoxic reactor than in the aerobic reactor, although the bio-cake layer deposited on the membrane surface in the anoxic reactor was thinner than that of the aerobic reactor. However, they disregarded that the two reactors had different microbial communities and mixed liquor suspended solids (MLSS) concentrations because the two reactors (aerobic and anoxic) were separated from each other. In reality, however, the microbial communities for either the m-BNR or the m-SBR processes would not necessarily change with the DO level to which the community is exposed. The aim of this study was to investigate the membrane filtration characteristics in a submerged MBR with intermittent aeration where the same microbial community is repeatedly exposed to alternating aerobic and anoxic conditions. Under these conditions, the permeability and structural changes of bio-cakes were investigated with DO level and operating time. Bio-cakes deposited on membrane surfaces were analyzed using confocal laser scanning microscopy (CLSM) and an image analysis technique.

Materials and Methods

MBR System. Figure 1 shows the schematic of the lab-scale submerged membrane bioreactor (MBR) used in this study. The MBR was operated under different aeration conditions as a function of time. The aerobic phase ran for 36 h, and subsequently, the anoxic phase also ran for 36 h. Therefore, total operation time for 1 cycle was 72 h with more than 12 cycles being repeated continuously. To change DO concentration while maintaining constant mixing intensity, 1 L/min of air was supplied to produce aerobic conditions (DO > 4.0 mg/L), whereas 1 L/min of nitrogen gas was supplied to create anoxic conditions (DO < 0.1 mg/L). The bioreactor, seeded with inoculum taken from a wastewater treatment plant, was fed with a synthetic wastewater containing 500 mg COD /L. HRT and SRT were 10 h and 20 days, respectively. The mixed liquor suspended solids (MLSS) concentration was kept between 4100 and 5700 mg/L throughout the operation.

Two hollow fiber membrane modules (membrane material: polyethylene, pore size: 0.4 μm, surface area of each membrane module: 0.03 m^2) were submerged into the bioreactor. One module was used for the analysis of the bio-cake structure and the other module was used for the quantitative analysis of attached biomass and bound EPS (extra-cellular polymeric substances) after detaching the bio-cake formed on the membrane surface. The MBR was operated under the constant flux of 8 L/m^2·h. Both modules were replaced by new ones at the end of each phase, which means that each module was used only for 36 h, except in special cases. For example, when the temporal variation of the bio-cake structure was monitored (section "Temporal Variation of Bio-Cake"), the membrane modules were run for 36 or 72 h.

* Corresponding author phone: +82-2-880-7075; fax: +82-2-874-0896; e-mail: leech@snu.ac.kr.
[†] Seoul National University.
[‡] Hoseo University.
[§] Korea Institute of Construction Technology.

10.1021/es070467a CCC: $37.00

Published on Web 07/28/2007

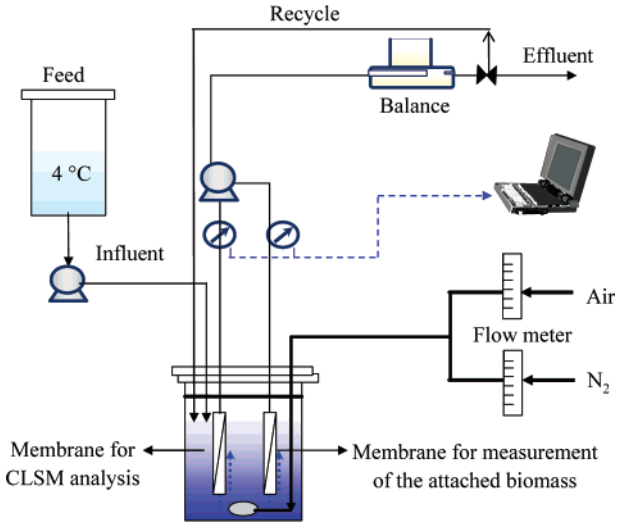

FIGURE 1. Schematic diagram of experimental setup.

Analysis. Chemical oxygen demand (COD) was determined by spectrometric methods (DR4000, Hach, Loveland, CO) with reagent kits (Hach). The turbidity of the supernatant, which was withdrawn after centrifugation (2000 rpm) of the mixed liquor for 5 min, was measured. Particle size distribution in the bulk phase was analyzed using a Master Sizer/E (Malvern, UK).

The extraction of the EPS from the bio-cake and microbial flocs in the bulk phase was done by a heating method after detaching the bio-cakes from the membrane surface into 200 mL of distilled water, as described by Park and Lee (*7*). Subsequently, the extract was analyzed for total polysaccharides and proteins, which are the major components of EPS. The sum of polysaccharides and proteins was expressed as the total EPS. Polysaccharides in the EPS were analyzed by the phenol-sulfuric acid method using glucose as a standard (*8*). Proteins were quantified using the Lowry method with a protein assay kit (Sigma, Germany) and bovine serum albumin (BSA) as a standard.

The molecular weight distribution of soluble components was measured by gel filtration chromatography (GFC, Waters, Milford, MA). An Ultrahydrogel 500 column (Waters) was used in conjunction with a refractive index detector (RID, Waters 2414). Filtered, degassed, and distilled water with 10 mM $NaNO_3$ was used as a mobile phase at a flow rate of 0.6 mL/min. Samples were filtered through 0.45 μm filters prior to injection to GFC.

Staining Bio-Cakes and Confocal Laser Scanning Microscopy (CLSM). A fraction of membrane fibers located in the middle section of the membrane module were cut out (length, 3 cm), and bacterial cells (e.g., bio-cakes) attached to those fibers were stained with a fluorescent dye, which is specific to bacterial cells. The bio-cakes were stained as described in other studies relevant to biofilm analysis using CLSM (*9*, *10*). The fluorescent dye SYTO 9 (excitation wavelength, 480 nm; emission wavelength, 500 nm; Molecular Probes, Eugene, OR), a cell-permeable nucleic acid dye, was used to visualize all cells. After the dye addition, the bio-cakes were incubated in darkness for 30 min at room temperature and then washed with a phosphate buffered saline (PBS) solution.

The stained bio-cakes were immediately observed by means of a confocal laser scanning microscope system (Radiance 2000, Bio-Rad, U.K.), which consisted of a microscope (Nikon TE 300, Japan) and krypton-argon mixed gas laser source. Signals were recorded in both the green channel (excitation 488 nm, emission 515/30 nm) and the red channel (excitation 568 nm, emission 600/50 nm). For the observation (magnification × 600), an oil lens of 60 × 1.4 NA was used. A series of CLSM images of optical sections with a step size of 1 μm were simultaneously taken from four random locations on each bio-cake specimen. The process was repeated until a total of 12 images were acquired for the three different bio-cakes. All images were stored and analyzed using image analysis programs.

Image Analysis. Two digital image analysis programs were used to obtain information on the architecture of the bio-cake layers. A commercial program, Image Structure Analyzer in 3-dimensions, ISA-2, was used to analyze the porosity and biovolume of the bio-cake. To visualize the 3D structure of bio-cake, CLSM images were reconstructed and presented as 3D views using IMARIS (v4.1.3, Bitplane AG, Zurich, Switzerland).

Results and Discussion

Membrane Permeability in an MBR Under an Intermittent DO Supply. The trans-membrane pressure (TMP) under constant flux mode was monitored as a function of time for each cycle. Two interesting phenomena were observed and are depicted in Figure 2a. First, the slope of the TMP increase in the anoxic phase was always steeper than in the aerobic phase regardless of cyclic number, indicating that the fouling was faster in the anoxic condition than it was in the aerobic. Second, the rate of TMP increase became higher as the cycles were repeated for both phases. However, this trend became less important as the cyclic number increased. For example, TMP increments from cycles 1 to 5 were much greater than those from cycles 5 to 12.

To elucidate the dependence of the rate of TMP increase on the DO concentration and cyclic number, structural analyses of the bio-cake layers formed on the membranes were carried out and compared. Figure 2b shows reconstructed CLSM images of bio-cake layers observed at the end of each phase and cycle. The bio-cake in the aerobic phase during the first cycle (cycle 1) was formed very sparsely, e.g., it did not cover the entire surface area of the membrane during the first 36 h of operation. After cycle 5, however, the surface was fully covered by the bio-cake. The thickness of a bio-cake layer also increased from 15 to 22 μm as the cyclic number went up from 1 to 12.

In the anoxic phase, however, the bio-cakes completely covered the membrane surface within the first 36 h, indicating that bio-cake formation rate in the anoxic phase was much higher than in the aerobic phase. Although the bio-cake layers became thicker as the cycles repeated, as they did in the aerobic phase, the increments of thickness from cycles 5 through 12 was negligible (37 to 39 μm). This coincided with the TMP increment mentioned above, i.e., the TMP increment from cycles 5 to 12 (or 5′ to 12′) was smaller than that from cycles 1 to 12 (1′ to 12′) as illustrated by Figure 2a.

It should be noted that the bio-cake formed in the anoxic phase was always thicker than that formed in the aerobic phase. However, the opposite observation, e.g., the bio-cake formed in the high DO reactor was thicker than that formed in the low DO reactor also was reported (*4*). This is because separate reactors were run in parallel having both a different DO and a different MLSS concentration. However, for this study we ran only one reactor with intermittent aeration, where we kept the same MLSS concentration.

The observation of reconstructed bio-cake images did not sufficiently explain the TMP profile. Further information on the architecture of the bio-cake, such as porosity and biovolume as well as on the amount of attached biomass, was required to fully elucidate the trends of TMP increase depicted in Figure 2.

Characteristics of the Bio-Cake Layer. Table 1 shows the comparison of bio-cake layers between aerobic and anoxic phases with respect to the total amount of attached biomass

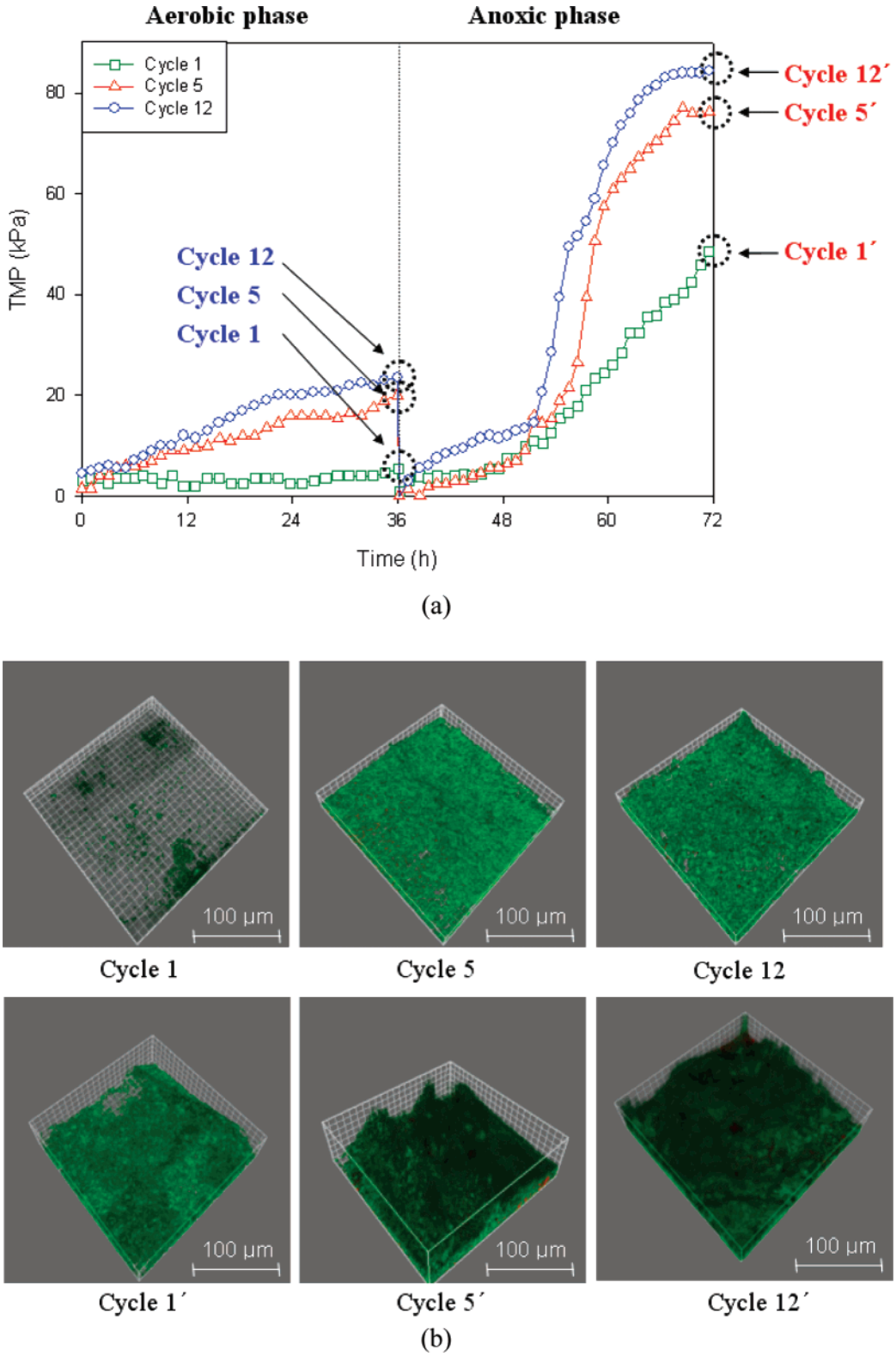

FIGURE 2. Comparison of (a) TMP profile and (b) bio-cake formation (bacterial cells) along with operation cycles.

(TAB) as well as porosity obtained from the CLSM image analysis. The porosity of the bio-cake calculated by CLSM would not directly reflect the real porosity of the bio-cake formed under pressurized condition because the pressure was released when the bio-cake specimen was detached from the membrane. According to the report by Park et al. (*11*), however, the bio-cake structure does not seem to change enough to worry about. They analyzed cake porosities formed during microfiltration of coagulated polystyrene latex bead suspension, and found that the porosities calculated using Carman−Kozeny equation and experimentally determined specific cake resistance under the pressure were similar to the porosities obtained using CLSM after detachment of the cake layer.

TAB accumulated on the membrane surface during the fixed filtration period (36 h) in the anoxic phase were always greater than in the aerobic phase, whereas porosity in the anoxic phase was always smaller than in the aerobic phase.

TABLE 1. Comparison of Porosity and Total Amount of Attached Biomass in Bio-Cake Layers between Aerobic and Anoxic Phases

	aerobic phase			anoxic phase		
	cycle 1	cycle 5	cycle 12	cycle 1′	cycle 5′	cycle 12′
TAB (mg)[a]	42	100	118	251	278	272
porosity	0.98 (±0.01)[b]	0.87 (±0.04)[b]	0.85 (±0.05)[b]	0.84 (±0.05)[b]	0.78 (±0.04)[b]	0.77 (±0.06)[b]

[a] TAB, total amount of attached biomass. [b] Standard deviation (n = 12).

The higher TAB and the lower porosity in the anoxic phase could be one of the reasons why the TMP increase in the anoxic phase was always steeper than in the aerobic phase.

For both phases, TAB increases and porosity decreases as the cycle numbers. Furthermore the differences of TAB and porosity between cycles 1 (1′) and 5 (5′) are greater than those between cycles 5 (5′) and 12 (12′). This coincides with the trend of TMP increase and bio-cake thickness discussed in the previous section. In summary, it can be concluded that the rate of TMP increase is in close association with the porosity and/or the TAB of a bio-cake layer. To generalize this conclusion, however, we need further information on the microbial community for each phase, because the differences in TMP rise-up might be attributed to differences in the microbial community. PCR−DGGE analysis showed that there was indeed no difference in the microbial community not only between the aerobic and anoxic phases, but also between the suspended and attached phases (data not shown). Consequently the potential effect of microbial diversity on membrane filterability could be excluded in the MBR under the repeated intermittent aeration.

Colloidal Particles. More often than not, the bio-cake properties in the MBR have been connected to the characteristics of the bulk-phase such as size of microbial flocs (*4*, *5*, *12*). These reports maintain that smaller floc size is one of the main causes for the reduced permeability in the anoxic phase compared with that in the aerobic phase. In this study, the mean particle size in the bulk phase showed about 110 and 100 μm in aerobic and anoxic phase, respectively. Although the microbial flocs in the anoxic phase were smaller than in the aerobic phase, there was no substantial difference in the mean floc size between the two phases throughout the cycles.

However, the mean particle size could not satisfactorily represent the influence of floc size on membrane filterability, because smaller particles have a greater impact on filterability. Therefore, a special quantitative analysis of small colloidal particles is needed. Unfortunately colloidal particles of less than 2 μm are not well detected by common particle size measuring instruments.

Since the correlation between the number of small particles and supernatant turbidity, e.g., the turbidity of the centrifuged bulk solution, was found to be very good (data not shown), we monitored the variation of supernatant turbidity as a function of operating time for both aerobic and anoxic phases. In the aerobic phase, there were no real differences in turbidity (5∼10 NTU) regardless of the cyclic number. Abrupt increases in turbidity to 25∼45 NTU were observed when the aerobic phase changed to the anoxic phase, which suggests the number of smaller particles increased at the phase switch.

During the anoxic phase, the microorganisms inside the flocs probably suffered from the restricted DO condition, this may have resulted in the enlargement of total area for the outer surfaces where a less competitive environment exists for DO uptake. Therefore, greater numbers of smaller flocs in the anoxic phase would give rise to higher turbidity and a less porous bio-cake formation than in the aerobic phase. This coincides with the porosity data in Table 1.

Soluble COD and EPS in the Bulk Phase. Soluble CODs, including EPS, are thought to be closely related to membrane biofouling in MBR processes. The soluble COD may represent all kinds of soluble foulants in the bulk solution. The soluble COD in the anoxic phase (200∼400 mg/L) was always higher than that in the aerobic phase (∼20 mg/L). Higher concentrations of soluble COD in the bulk phase should accelerate TMP increase because soluble COD components, especially EPS, could reduce the porosity of the bio-cake layer due to the adsorption and a filling of the interstitial pores in the bio-cake layer. The higher concentrations of soluble COD in the anoxic phase would have two origins: undigested feed components and EPS excreted from microorganisms. Since the heterotrophic microbes lost their activity in the anoxic condition, feed components could not be metabolized satisfactorily. Moreover, microorganisms in an activated sludge process tend to excrete more EPS to cope with a lower DO environment (*12*). This is in agreement with Drews et al. (2007) who found that the net elimination of soluble EPS decreased, i.e., the concentration of soluble EPS rose, when DO and nitrate concentrations were low.

The soluble EPS concentrations, expressed as the sum of polysaccharides and proteins, were 4∼12 mg/L in the aerobic phase and 34∼51 mg/L in the anoxic phase. However, determination of the soluble EPS concentration excreted only from microorganisms was impossible because protein-like substances were also included in the synthetic feed. Therefore, a GFC of the bulk solution was carried out to confirm the origin of the soluble EPS in the bulk phase. The chromatograms (Figure 3) show the soluble components (e.g., EPS) contained in the feed (Figure 3a), in both the aerobic and anoxic bulk phases (Figure 3b) and in the permeate (Figure 3c) at cycle 12. It is worth noting that the peak near 8 min of retention time in the anoxic phase corresponds to the molecular weight of about 2 000 000D was detected neither in the feed (Figure 3a) nor in the aerobic phase (Figure 3b). As a result, the peak was believed to represent the fraction of the soluble EPS that were excreted from the microorganisms in the anoxic phase. Moreover, this peak was not detected in the permeate (Figure 3c), suggesting that those macromolecules were removed by adsorption to the bio-cake layer and/or to the membrane itself. This particular EPS may aggravate membrane biofouling and thus increase the TMP increase rate in the anoxic phase as illustrated in Figure 2a.

Bound EPS in the Bulk Phase and in the Bio-Cake Layer. There may be two kinds of EPS in a MBR: (i) soluble EPS in the bulk phase, and (ii) bound EPS that are embedded in the microbial flocs in the bio-cake layer as well as in the bulk phase. Since the bound EPS provides a highly hydrated gel matrix in which microorganisms are embedded, they are considered to be a significant hydraulic barrier to permeate flow through the bio-cake layer. Therefore, quantitative determination of the bound EPS was required to explain the membrane biofouling.

Figure 4a shows the variation of bound EPS in the bulk phase. The amount of bound EPS per unit microorganism was similar in the aerobic and anoxic phases during cycle 1 (1′). However, the bound EPS concentrations in the anoxic

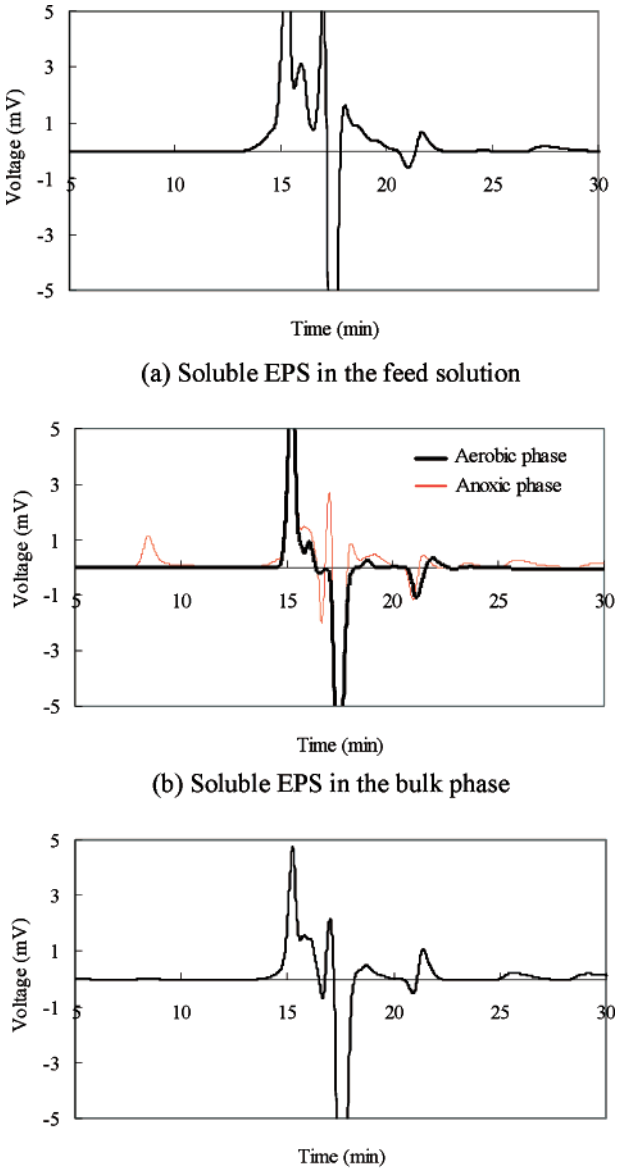

FIGURE 3. GFC spectrum of soluble EPS components in the feed solution, bulk phase, and permeate.

phase became smaller than those in the aerobic phase during cycles 5 (5′) and 12 (12′). This phenomenon seems to be closely related to the change in the floc structure. The microbial flocs in the bulk phase are comprised of bound EPS and microbial colloidal particles. When the aerobic phase changed to anoxic, parts of colloidal particles and bound EPS were released from the flocs as discussed in the previous section, "Colloidal Particles." Thus, the bound EPS inside the flocs decreased, whereas the turbidity and soluble COD in the bulk solution increased as discussed previously.

In contrast to the bulk phase, however, the bound EPS concentrations in the bio-cake layer were unexpectedly similar in the two phases as illustrated by Figure 4b. As mentioned in the section, "Soluble COD and EPS in the Bulk Phase," the soluble EPS concentration was higher in the anoxic phase (34∼51 mg/L) than it was in the aerobic phase (4∼12 mg/L). During filtration, the soluble EPS in the bulk phase should move toward the membrane surface and be intermingled into the bio-cake layer, which could explain the bound EPS concentrations in the bio-cake layer becoming similar in the two phases. In addition, the fouling rate in

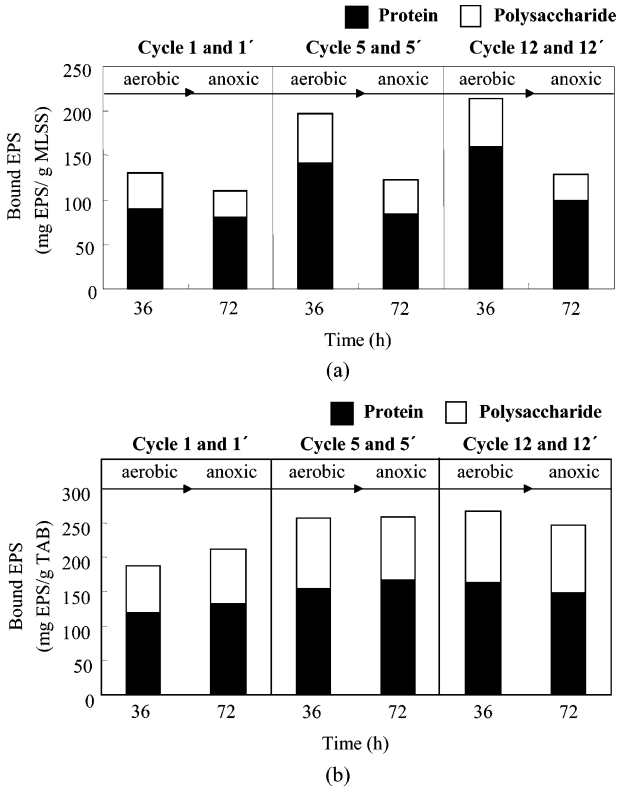

FIGURE 4. Variations in the bound EPS concentration: (a) in the bulk phase; (b) in the bio-cake.

aerobic phase coincided well with the variation of the bound EPS concentration in the bio-cake.

Temporal Variation of Bio-Cake. The architectural features of the bio-cake layer, such as porosity and biovolume, are in close association with its specific resistance and thus directly related to the membrane permeability in an MBR. Consequently, it would be interesting to monitor the spatial and temporal changes in the architecture of bio-cake layer with operation time for both aerobic and anoxic phases.

Various bio-cakes were formed under different oxygen conditions and each bio-cake was analyzed in terms of porosity and biovolume, then compared for spatial and temporal changes in architecture. The results are summarized in Table 2 and Figure 5:

(a) Bio-cake 1, formed only under aerobic conditions for 36 h.

(b) Bio-cake 2, formed only under anoxic conditions for 36 h.

(c) Bio-cake 3, formed under aerobic conditions for 36 h and anoxic conditions for another 36 h (total 72 h).

(d) Bio-cake 4, formed only under anoxic conditions for 72 h.

(e) Bio-cake 5, formed under anoxic conditions for 36 h and aerobic conditions for another 36 h (total 72 h).

Table 2 shows that the bio-cake 1 which formed for 36 h under aerobic conditions has a larger porosity and smaller biovolume than the bio-cake 2 which formed for the same time in an anoxic phase. On the other hand, the bio-cake 3 formed for 72 h: 36 h under aerobic conditions and another 36 h under anoxic conditions. Consequently, it was expected that the lower part of the bio-cake 3, which was formed under the aerobic conditions, would be more porous than the upper part, which was formed under anoxic conditions. Unexpectedly, however, the porosity profiles along the depth of the bio-cake layers were quite similar to each other as detailed in Figure 5a. Moreover, the porosity of the lower part of the bio-cake 3 was even smaller than that of the bio-cake 2.

TABLE 2. Comparison of the Average Porosity and Biovolume of Bio-Cakes Formed under Various Filtration Conditions

	average porosity	biovolume ($\times 10^6$ μm^3)	filtration time	TMP (kPa) at the end of run
bio-cake 1	0.85 ($\pm$0.06)[a]	0.9 ($\pm$0.6)[a]	36 h (aerobic)	16
bio-cake 2	0.75 ($\pm$0.03)[a]	2.9 ($\pm$0.5)[a]	36 h (anoxic)	75
bio-cake 3	0.71 ($\pm$0.03)[a]	3.6 ($\pm$0.5)[a]	72 h (aerobic 36 h + anoxic 36 h)	86
bio-cake 4	0.68 ($\pm$0.05)[a]	4.4 ($\pm$0.6)[a]	72 h (anoxic)	96
bio-cake 5	0.70 ($\pm$0.05)[a]	3.9 ($\pm$0.9)[a]	72 h (anoxic 36 h + aerobic 36 h)	89

[a] Standard deviation (n = 12).

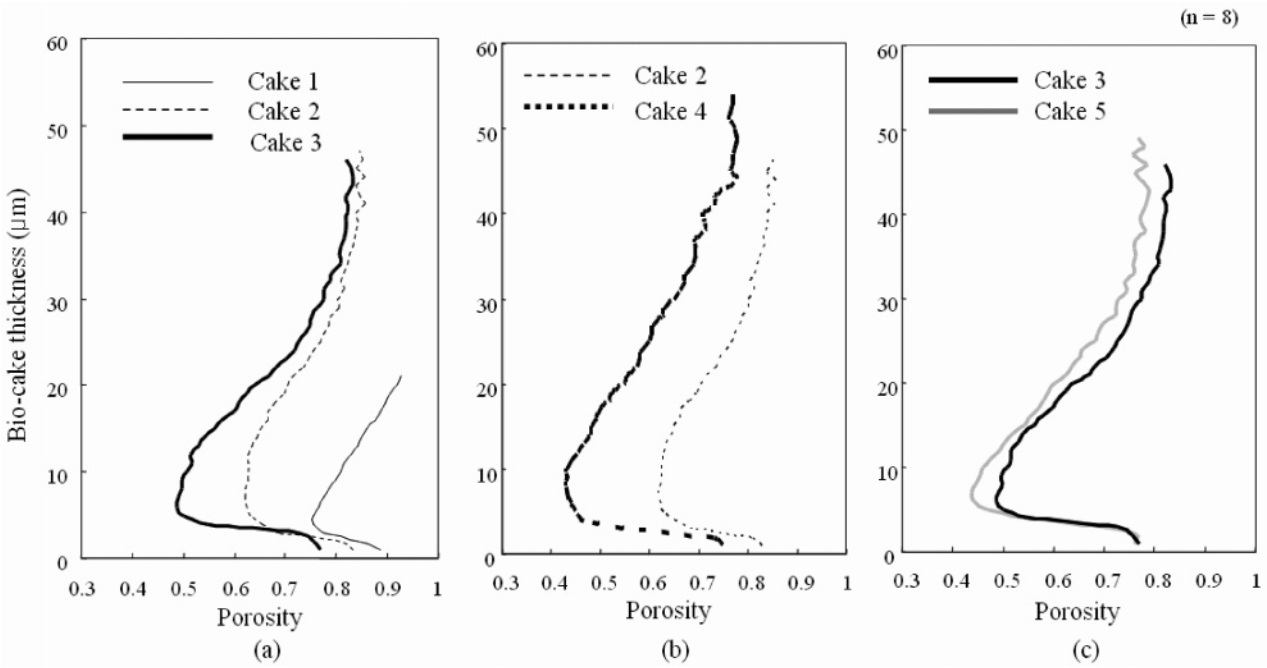

FIGURE 5. Porosity profiles along the bio-cake depth.

Several answers may explain this unexpected phenomenon. First, the lower part of the bio-cake 3 already formed under the 36 h of aerobic conditions could be altered from a porous to a dense architecture during the next 36 h of anoxic conditions. Since we found that smaller colloidal particles and soluble COD are released from the microbial flocs during anoxic conditions, the lower part of the bio-cake 3 would be exposed to this newly changed circumstance. If so, the lower part could become less porous during the 36 h of anoxic conditions as the smaller colloidal particles and soluble COD blocking the pores of the bio-cake that was preformed during the first 36 h of aerobic conditions. Second, the lower part of the bio-cake 3 had been compressed for a longer time (72 h) than that of the bio-cakes 1 and 2 (each for 36 h). As a result, it had changed to a structure that was more dense due to the compression under the higher TMP.

To verify which factor is more prevalent, two other bio-cakes (bio-cake 4 and 5 in Table 2) were prepared and examined. Bio-cakes 2 and 4 were formed at the identical anoxic condition, but bio-cake 4 was exposed to the TMP for two times longer than the bio-cake 2. Table 2 shows that the bio-cake 4 (average porosity: 0.68, biovolume: 4.4×10^6 μm^3) has greater biovolume, but is less porous than the bio-cake 2 (average porosity; 0.75, biovolume; 2.9×10^6 μm^3). Because the bio-cake 4 was exposed to the greater TMP at twice the time period as the bio-cake 2, the bio-cake 4 should be compressed more. As shown in Figure 5b, the porosity profile of the bio-cake 4 is shifted to the left compared to that of the bio-cake 2 throughout the depth. This strongly supports the theory that the greater compression is due to an elongated duration and a greater TMP for the bio-cake 4.

On the other hand, comparing the bio-cake 3 and 5 under the same duration, but with a reversed DO regime, there was little difference in either the biovolume or the porosity (Table 2 and Figure 5c). This suggests that the sequence of the DO regime is not so critical for the bio-cake architecture, i.e., the order of the DO condition has little impact on that. Consequently, compression is the most important factor determining temporal and spatial variation in the bio-cake architecture.

Acknowledgments

We thank the Korean Ministry of Science and Technology for their financial support under grant M6-0403-00-0098. We also thank the Korean National Instrumentation Center for Environment Management (NICEM) for the use of the confocal laser scanning microscope system.

Literature Cited

(1) Drews, A.; Kraume, M. Process improvement by application of membrane bioreactors. *Trans. Inst. Chem. Eng., Chem. Eng. Res. Des.* **2005**, *83* (A3), 276−284.

(2) Kraume, M.; Bracklow, U.; Vocks, M.; Drews, A. Nutrients removal In MBRs for municipal wastewater treatment. *Water Sci. Technol.* **2005,** *51*, 391−402.

(3) Kang, I. J.; Lee, C. H. Effect of aerobic period on microfiltration performance in a membrane-coupled sequencing batch reactor. *J. Ind. Eng. Chem.* **2004**, *10* (1), 146−151.

(4) Jin, Y. L.; Lee, W. N.; Lee, Lee, C. H.; Chang, I. S.; Huang, X.; Swaminathan, T. Effect of DO concentration on biofilm structure and membrane filterability in submerged membrane bioreactor. *Water Res.* **2006**, *40* (15), 2829−2836.

(5) Yun, M. A.; Yeon, K. M.; Park, J. S.; Lee, C. H. Characterization of biofilm structure and its effect on membrane permeability in MBR for dye wastewater treatment. *Water Res.* **2006**, *40*, 45−52.

(6) Drews, A.; Mante, J.; Iversen, V.; Vocks, M.; Lesjean, B.; Kraume, M. Impact of ambient conditions on SMP elimination and rejection in MBR. *Water Res.* **2007**, doi:10.1016/j.watres.2007.05.046.

(7) Park, J. S.; Lee, C. H. Removal of soluble COD by a biofilm formed on a membrane in a jet loop type membrane bioreactor. *Water Res.* **2005**, *39* (19), 4609−4622.

(8) Dubois, M.; Gilles, K. A.; Hamiltin, J. K.; Rebers, P. A.; Smith, F. Colorimetric method for determination of sugars and related substances. *Anal. Chem.* **1956**, *28*, 350−356.

(9) Neu, T. R.; Swerhone, G. D. W.; Lawrence, J. R. Assessment of lectin-binding analysis for in situ detection of glycoconjugates in biofilm systems. *Microbiology* **2001**, *147*, 299−313.

(10) Strathmann, M.; Wingender, J.; Flemming, H. C. Application of fluorescently labeled lectins for the visualization and biochemical characterization of polysaccharides in biofilm of *Pseudomonas aeruginosa*. *J. Microbiol. Methods* **2002**, *50*, 237−248.

(11) Park, P. K.; Lee, C. H. Determination of cake porosity using image analysis in a coagulation-microfiltration system. *J. Membr. Sci.* **2007,** *293*, 66−72.

(12) Kim, H. Y.; Yun, K. M.; Lee, C. H.; Lee, S. H.; Swaminathan, T. Biofilm structure and extracellular polymeric substances in low and high dissolved oxygen membane bioreactors. *Sep. Sci. Technol.* **2006**, *41*, 1213−1230.

Received for review February 23, 2007. Revised manuscript received June 17, 2007. Accepted June 19, 2007.

ES070467A